Measurement of the Positive Muon Lifetime to 1 ppm

David M. Webber*

University of Illinois, Urbana-Champaign

Advisor: David W. Hertzog (Dated: March 31, 2005)

Abstract

The goal of my thesis experiment is a measurement of the positive muon lifetime (τ_{μ}) to a precision of one part per million. The muon lifetime provides the most precise determination of the Fermi coupling constant, G_F , which is one of the fundamental inputs to the Standard Model. Recent advances in theory have reduced the theoretical uncertainty on G_F as calculated from the muon lifetime to a few tenths of a ppm. The remaining uncertainty on G_F is entirely experimental, and is dominated by the uncertainty on τ_{μ} . The muon lifetime, however, has not been updated in over 20 years. The ongoing Muon Lifetime Analysis (MuLan) experiment will use an innovative pulsed beam, a symmetric 3π detector, and modern data-taking methods to reduce the uncertainty on τ_{μ} to 1 ppm. Given the upcoming capabilities of the MuLan detector and the fundamental nature of G_F , an updated measurement of the muon lifetime must be attempted.

^{*}Electronic address: dwebberQuiuc.edu

Parameter	Determined by	Value	$\delta G_F \; (\mathrm{ppm})$
$ au_{\mu}$	muon lifetime [2]	$2.17903(4)~\mu s$	9
m_{μ}	comparison with mass of a nucleus [2]	0.1134289264(30) u	0.06
$m_{ u_{\mu}}$	$\pi^+ \to \mu^+ + \nu_\mu \text{ decay } [2]$	${<}190~\rm{keV}$	13
$m_{ u_{\mu}}$	precision cosmology [2]	$\Sigma_i m_{\nu_i} < 0.71 \text{ eV}$	negligible
η	experiment, general analysis [1]	$(71 \pm 37 \pm 5) \times 10^{-3}$	360
η	experiment, restricted analysis [1]	$(-2.1 \pm 7.0 \pm 1.0) \times 10^{-3}$	68
η	standard model	0	0

Table I: Experimental contributions to δG_F . If we neglect the muon neutrino mass or believe recent cosmological results, the muon lifetime gives the dominant uncertainty on G_F . The values for η come from a dedicated experiment at PSI [1], but under the Standard Model η is expected to be 0.

I. INTRODUCTION

The Fermi coupling constant, G_F , when combined with the fine structure constant, α , and the mass of the Z-boson, m_Z , is one of the most precise inputs of the Standard Model. The muon lifetime provides the most sensitive determination of G_F because the muon decay involves only fermions and is believed to occur only though electroweak processes. Recent work by Ritbergen and Stuart [6] has reduced the theoretical uncertainty on the extraction of G_F from the muon lifetime to a few tenths of a ppm, so the remaining uncertainty δG_F is entirely experimental. The dominant uncertainty on G_F comes from

$$\frac{\delta G_F}{G_F} = -\frac{1}{2} \frac{\delta \tau_{\mu}}{\tau_{\mu}} - \frac{5}{2} \frac{\delta m_{\mu}}{m_{\mu}} + 4 \frac{m_{\nu_{\mu}}^2}{m_{\mu}^2}.$$

Recent results from the cosmological sector suggest the sum of all neutrino masses is below 1 eV, so we can safely neglect the third term. It is clear from table I that the dominant uncertainty on G_F comes from the muon lifetime. The current value of G_F , sometimes referred to as G_{μ} when extracted from the muon lifetime, is known to 9 ppm,

$$G_{\mu} = 1.16639(1) \text{ GeV}^{-2}.$$

The goal of my doctoral research will be to reduce the uncertainty on the muon lifetime by a factor of ≈ 20 to 1 ppm, and consequently the uncertainty on G_F to 0.5 ppm.

II. THEORY

A. Extracting G_F from the muon lifetime

For historical reasons, the muon decay is often written in terms of a four-fermion point interaction. Assuming the neutrinos involved are left-handed Dirac fermions, the Lagrangian for the weak Fermi contact interaction can be written

$$\mathcal{L}_W = -2\sqrt{2}G_F[\bar{\psi}^0_{\nu_\mu}\gamma_\lambda\gamma_L\psi^0_\mu] \cdot [\bar{\psi}^0_e\gamma_\lambda\gamma_L\psi^0_{\nu_e}],$$

where ψ^0_μ , ψ^0_e , $\psi^0_{\nu_\mu}$, and $\psi^0_{\nu_e}$ are the bare wave functions of the muon, electron, muon neutrino, and electron neutrino, respectively. Here, $\gamma_L=1-\gamma_5$ is the left-handed Dirac projection operator and γ_λ are the familiar gamma matrices. This reaction is often referred to as a "V-A" interaction since we can rewrite

$$\bar{\psi}\gamma_{\lambda}\gamma_{L}\psi = \bar{\psi}\gamma_{\lambda}\psi - \bar{\psi}\gamma_{\lambda}\gamma_{5}\psi$$

showing the Lagrangian is composed of vectors minus axial-vectors.

For completeness, the quantum electrodynamic (QED) and quantum chromodynamic (QCD) Lagrangians should be added to the muon-decay Lagrangian, giving

$$\mathcal{L}_F = \mathcal{L}_{\text{QED}}^0 + \mathcal{L}_{\text{QCD}}^0 + \mathcal{L}_W.$$

From L_F one obtains to leading order in G_F

$$\frac{1}{\tau_{\mu}} \equiv \Gamma_{\mu} = \Gamma_0 (1 + \Delta q),$$

where $\Gamma_0 = \frac{G_F^2 m_\mu^5}{192\pi^3}$ and τ_μ is the muon lifetime. The radiative corrections are given by $\Delta q = \sum_{i=0}^{\infty} \Delta q^{(i)}$, where *i* gives the number of times the renormalized coupling constant evaluated at the muon mass,

$$\alpha_r(m_\mu)^{-1} = \alpha^{-1} - \frac{2}{3\pi} \ln\left(\frac{m_e}{m_\mu}\right) + \frac{1}{6\pi} \sim 136,$$

appears in these corrections. The first three terms have been calculated and are given by

$$\Delta q^{(0)} = -8x - 12x^2 \ln x + 8x^3 - x^4 - 8y + \mathcal{O}(xy)$$

$$\Delta q^{(1)} = \left(\frac{\alpha_r}{\pi}\right) \left(\frac{25}{8} - 3\zeta(2) - (34 + 12\ln x)x + 96\zeta(2)x^{\frac{3}{2}} + \mathcal{O}(x\ln^2 x)\right)$$

$$\Delta q^{(2)} = \left(\frac{\alpha_r}{\pi}\right)^2 \left(\frac{156815}{5184} - \frac{1036}{27}\zeta(2) - \frac{895}{36}\zeta(3) + \frac{67}{8}\zeta(4) + 53\zeta(2)\ln 2 - (0.042 \pm 0.002)\right)$$

where $x = \frac{m_e^2}{m_\mu^2}$, $y = \frac{m_{\nu_\mu}^2}{m_\mu^2}$, and ζ is the Riemann zeta function. The remaining uncertainty on G_F should not exceed a few tenths of a ppm [6].

One can extract G_F from τ_{μ} using the relations summarized in [5], which states

$$\tau_{\mu}^{-1} \equiv \Gamma(\mu \to \text{all}) = \frac{G_F^2 m_{\mu}^2}{192\pi^3} f\left(\frac{m_e^2}{m_{\mu}^2}\right) (1 + \text{R.C.}) \left(1 + \frac{3}{5} \frac{m_{\mu}^2}{m_W^2}\right).$$

Here, m_{μ} , m_e , m_W are the muon, electron, and W-boson masses, respectively and f(x) is given by

$$f(x) = 1 - 8x + 8x^3 - x^4 - 12x^2\ln(x).$$

The radiative corrections (R.C.) are given by

R.C. =
$$\frac{\alpha}{2\pi} \left(\frac{25}{4} - \pi^2 \right) \left(1 + \frac{\alpha}{\pi} \left(\frac{2}{3} \ln \frac{m_{\mu}}{m_e} - 3.7 \right) + \left(\frac{\alpha}{\pi} \right)^2 \left(\frac{4}{9} \ln^2 \frac{m_{\mu}}{m_e} - 2.0 \ln \frac{m_{\mu}}{m_e} + C \right) + \dots \right).$$

Here, α is the renormalized fine structure constant, $\alpha^{-1}(0) = 137.03599911(46)$.

Considering that theory has surpassed experiment, reducing the uncertainty on G_F to a term dependent only on the muon lifetime, and that the last experimental value was produced in 1984, it is time for an updated measurement of the muon lifetime.

B. Properties of the muon decay

If we consider muon decay as a four-fermion "V-A interaction" and neglect radiative corrections, neutrino masses, and terms of order $x_0^2 = [2m_e m_\mu/(m_\mu^2 + m_e^2)]^2$, the angular and energy distributions of the decay positron follow

$$\frac{d^2\Gamma}{dx\,d\cos\theta} \sim x^2 \left(3(1-x) + \frac{2\rho}{3}(4x-3) + 3\eta x_0 \frac{(1-x)}{x} + P_\mu \varepsilon \cos\theta \left(1 - x + \frac{2\delta}{3}(4x-3) \right) \right) \tag{1}$$

where the reduced energy $x = 2E_e m_\mu/(m_\mu^2 + m_e^2)$ and the parameters $\{\rho, \eta, \varepsilon\}$ are Michel parameters determined to be $\{\frac{3}{4}, 0, 1\}$ under the Standard Model [2]. The MuLan detector is not sensitive to energy, but the angular distribution plays an important role. Integrating over energy and inserting the Michel parameters from the Standard Model, we find

$$\frac{d\Gamma}{d\cos\theta} = \frac{G_F^2 m_\mu}{192\pi^2} \left(\frac{1}{2} + \frac{1}{6} P_\mu \cos\theta\right). \tag{2}$$

One important disclaimer must be made about the η term appearing in equation 1. Under the Standard Model, η is assumed to be 0, but the value of η can also be tested experimentally. Using

Experiment	Facility	Measurement	Physics	
TWIST	Triumf	polarized muon decay	Michel parameters ρ , δ , $(P_{\mu}\xi)$	
FAST	PSI	muon decay from stopped pions	Fermi constant G_F	
MuCap	PSI	muon capture on proton	pseudoscalar form factor g_p	
MuLan	PSI	muon decay from stopped muons	Fermi constant G_F	
(unnamed)	Riken-Ral	muon decay from stopped muons	Fermi constant G_F	
MECO	BNL	$\mu \to e \text{ conversion}$	lepton flavor violation	
MEGA	LANL	$\mu \to e + \gamma$	lepton flavor violation	
MEG	PSI	$\mu \rightarrow e + \gamma$	lepton flavor violation	
g-2	BNL	muon spin precession	anomalous muon magnetic moment	
(unnamed)	PSI	decay positron polarization	Michel parameter η	
SINDRUM	SIN	$\mu^+ \to e^+ + e^+ + e^-$	lepton flavor violation	
SINDRUM II	PSI	$\mu^+ \to e^+ + e^+ + e^-$	lepton flavor violation	
(unnamed)	PSI	$\mu^+e^- \to \mu^-e^+$	lepton flavor violation	

Table II: An incomplete list of past and present experiments studying muon decay [3].

the most general four-fermion point-interaction model, η takes the form

$$\eta = \frac{1}{2} \operatorname{Re} \{ g_{LL}^V g_{RR}^{S*} + g_{RR}^V g_{LL}^{S*} + g_{LR}^V (g_{RL}^{S*} + 6g_{RL}^{T*}) + g_{RL}^V (g_{LR}^{S*} + 6g_{LR}^{T*}) \}$$
 (3)

where $g_{\varepsilon\mu}^{\gamma}$ are the electroweak coupling constants, L and R stand for left- and right-handed couplings, and $\{S,V,T\}$ stand for scalar, vector, and tensor couplings. The Standard Model predicts $g_{LL}^{V}=1$ and all other $g_{\varepsilon\mu}^{\gamma}=0$, so if equation 3 is restricted to neglect terms of order 2 and higher containing nonstandard couplings, $\eta=\text{Re}\{g_{RR}^{S}/2\}$. The general analysis yields the experimental value $\eta=(71\pm37\pm5)\times10^{-3}$, whereas the restricted analysis yields $\eta=(-2.1\pm7.0\pm1.0)\times10^{-3}$. Since

$$G_F pprox G_F^{V-A} \left(1 - 2\eta \frac{m_e}{m_\mu} \right),$$

these values increase δG_F by factors of 40 and 7.6, respectively (see table I) [1].

III. EXPERIMENTAL METHOD

The muon lifetime is found by fitting an exponential to a histogram formed from the time differences between when a muon comes to rest and when it decays. In an idealized model, where there are no background events from cosmic rays or other sources, the shape of the histogram is

an exponential and the only unknown parameters are the number of events and the lifetime. If the number of events is large enough that Gaussian statistics can be assumed, the fractional uncertainty on the lifetime is

$$\frac{\delta \tau_{\mu}}{\tau_{\mu}} = K \frac{1}{\sqrt{N_0}}.\tag{4}$$

Therefore, to get a statistical accuracy of 1 ppm on the muon lifetime, it is necessary to record on the order of K^210^{12} events. The proportionality constant, K, in equation 4 depends on the nature of the fit. In the idealized case mentioned here, K = 1. Given a more complicated fit function including a flat background, an uncertain number of events, a "wiggle" term from muon precession, and a pileup term from missed events, the proportionality constant will increase as data is "consumed" by these other functions. Numerical simulations suggest that K lies between 2 and 4, not taking into account the background term [4].

The $\mathcal{O}(10^{12})$ events necessary for a measurement of the muon lifetime to 1 ppm requires a different method for measuring the muon lifetime than "one at a time." Rather than a slow beam rate of roughly 20 kHz, where one muon is present in the target at a time, MuLan will run in a high-rate, kicked-beam mode where the target is "loaded" with muons over a period of 5 μ s. After the incoming muon beam is switched off, the surviving muons in the target are allowed to decay for a period of ten or more muon lifetimes. Unfortunately, there are no periodic muon beams with a time structure of 5 μ s on, 27 μ s off, so we chose to use a continuous muon beam and introduce the necessary chopped beam structure with an electrostatic kicker.

During "loading," low-energy "surface muons" stop in a depolarizing target surrounded by a "soccer ball" composed of scintillator tiles, which detect outgoing positrons. Filling a histogram with time differences between the kicker beam-off transition and the times of hits in the ball gives a decay exponential with the characteristic time of the muon lifetime.

IV. BEAMLINE AND TARGET

The MuLan experiment utilizes the piE3 beamline at the Paul Scherrer Institute (PSI) in Villigen, Switzerland (Fig 1). PSI's main ring proton accelerator typically runs at 1.8 mA, making it the most intense dc proton beam in the world. The protons are guided through a carbon target where roughly 40-60% of the protons react to produce pions. The piE3 beamline is tuned to accept $\approx 28 \text{ MeV}/c$ "surface muons" coming from pions that decay at rest near the surface of the target. The beamline takes a vertical step of five meters using opposing 60 degree bends up to the second

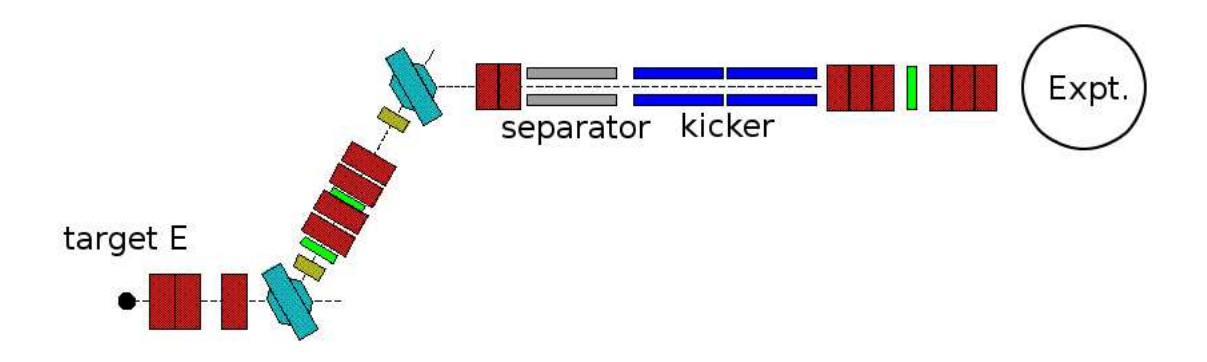


Figure 1: The piE3 beamline at the Paul-Scherrer Institute as used by the MuLan experiment (not to scale). Red boxes represent quadrupole magnets, yellow represent sextapoles, and green represent slits. The proton beam incident on target E points perpendicular to the page.

floor, where an $E \times B$ separator reduces the number of positrons in the beam. The separator is followed by an electrostatic kicker composed of two sets of parallel horizontal plates. The kicker is controlled by a programmable gate generator and can switch from 0 V to 25 kV across the plates in 45 ns with a maximum operating frequency of 50 kHz. Current beamline and kicker settings give a muon extinction factor, defined by the beam-on rate over the beam-off rate, of about 300.

Downstream of the kicker is a focusing quadrupole triplet, a slit, and another triplet. At the end of the beampipe is a 100 μ m mylar window marking the muon's exit from vacuum into air. Immediately after the vacuum window, there is an entrance muon counter (EMC) composed of x and y wire planes surrounded by a fast gas of 70% CF₄ and 30% isobutane. Each plane has 96 wires, which are read out in pairs by preamplifying pulse-shaping discriminators [7] and TDCs. Following the EMC, a helium bag reduces premature stopping by lowering the density of the gas the muons must traverse before they reach the target. The stopping target is either sulfur or Arnokrome-3 (30% chromium, 10% cobalt, 60% iron) (AK-3). The sulfur target is naturally depolarizing and is surrounded by rare-earth magnets in a Halbach configuration, which approximates a uniform 150 G field. The AK-3 target has an internal field of 0.5 Tesla, which precesses the muons faster than the time-resolution of our electronics.

V. DETECTOR

A. Hardware

Surrounding the target is the MuLan detector ball, which is a truncated icosahedron (soccer ball) with twenty hexagonal faces and twelve pentagonal faces [Fig 3]. Two pentagonal faces have

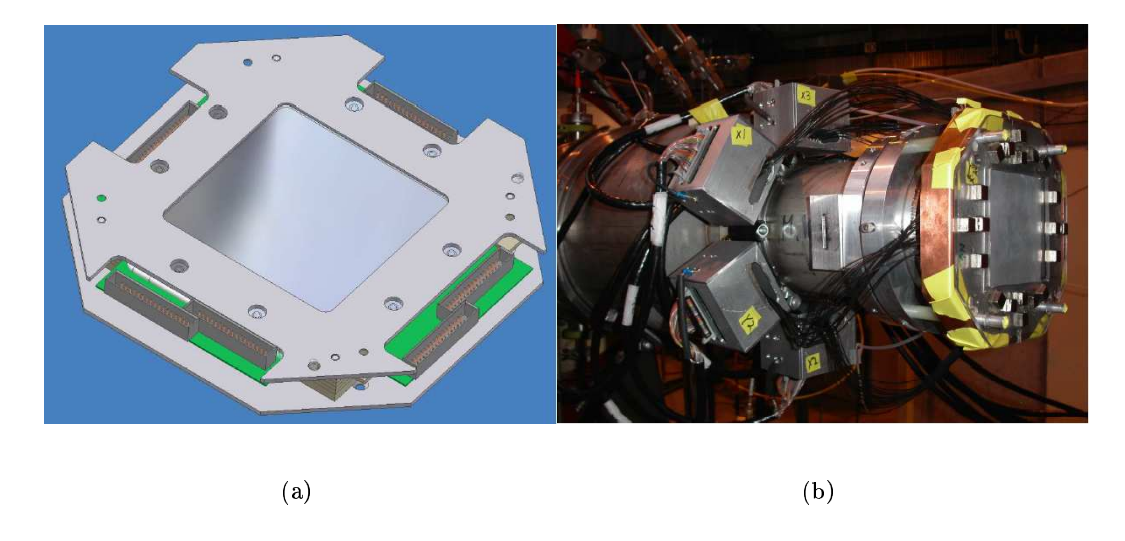


Figure 2: The entrance muon counter (EMC) is a multiwire proportional counter attached to the end of the beampipe. It has 96 x- and 96 y-wires which are read out in pairs, giving 2 mm accuracy on the beam position. On the left is a schematic drawing of the EMC. On the right is the EMC in situ, identified by the copper plating on the side. The readout electronics are attached to a collar around the beampipe. An array of magnets attached downstream of the EMC ensures the few $(\mathcal{O}(10^{-3}))$ muons that stop in the EMC precess in a 75 G field or higher.

been removed to allow beam entrance and exit. Each face is composed of triangular scintillator tiles, six pairs in the hexagonal faces and five in the pentagonal faces. The pairs are nested as "inners" and "outers" so that a coincidence between the pairs indicates a particle traversed the surface of the ball [Fig 4a]. Taking into account the missing pentagons and space between the tiles, the detector provides roughly 3π coverage of the target.

Phototubes attached to each tile convert the scintillation light to an amplified electrical pulse. In the current setup, the analog signals are discriminated and sent to time digitizers (TDCs). The output of the time digitizers is recorded directly to disk. In 2005, we will begin testing waveform digitizers (WFDs) in parallel with the TDCs. Although the WFDs will provide better pulse characterization resulting in superior noise suppression, the increase in data volume will introduce some new challenges in recording and analyzing the data. It is hoped that a significant dataset using WFDs can be taken in the fall, and that the full dataset will be taken in 2006.

B. Software

Data acquisition (DAQ) is handled by MIDAS, a data acquisition system for small to medium sized physics experiments [8]. A complete DAQ system is composed of MIDAS libraries and utilities

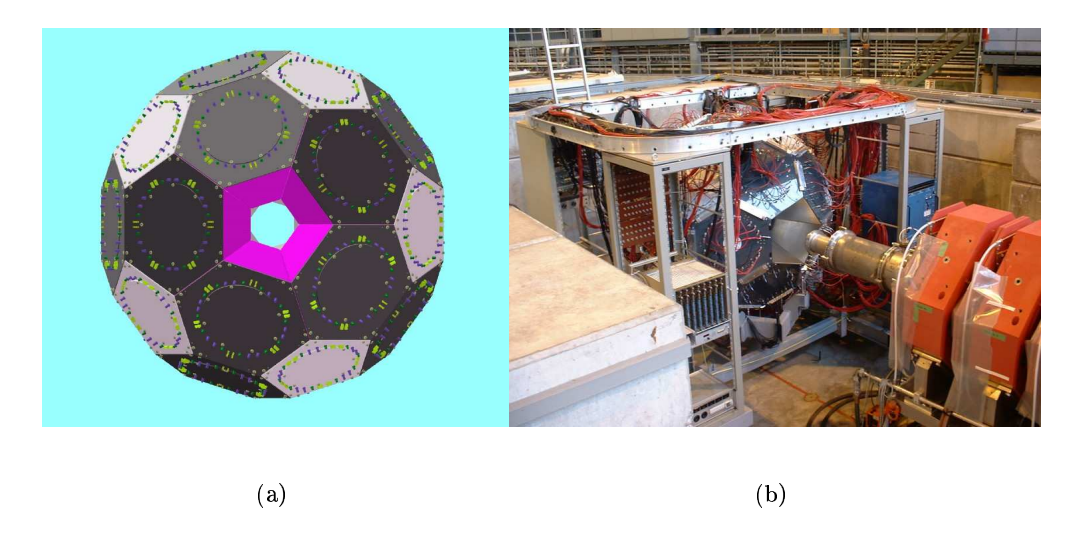


Figure 3: The MuLan detector is composed of 170 nested pairs of scintillating triangular tiles, giving 3π coverage of a central depolarizing target. (a) An engineering drawing of the detector housing. The detector is composed of twenty hexagonal and ten pentagonal detector houses. The muon beam points into the page. (b) The MuLan detector cabled and in position in the piE3 beam area at Paul Scherrer Institute, Switzerland.

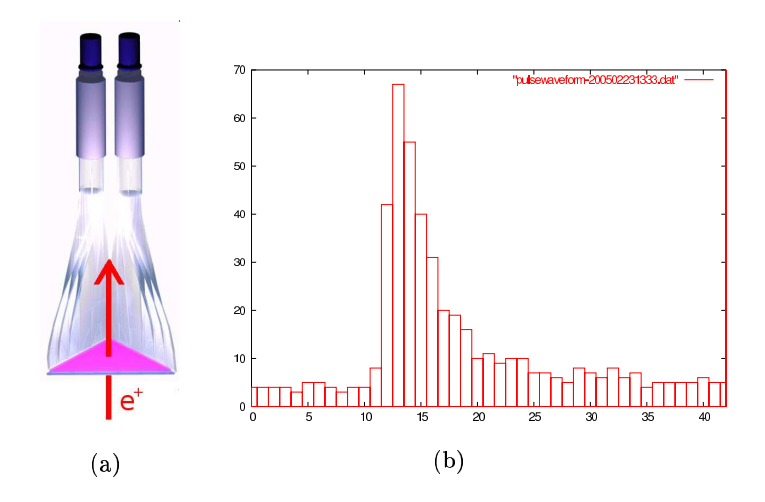


Figure 4: (a) Nested inner and outer triangular tiles. Each triangular scintillator tile (purple) has a light guide attached to one edge, which adiabatically transports the light to a phototube. (b) A phototube pulse digitized by the prototype waveform digitizer.

combined with user readout and analysis code. In the MuLan experiment, six frontend machines will record data directly from the WFDs using a PCI-VME interface. The data will be examined to remove bad pulses, compressed, and passed over gigabit ethernet to the backend machine for storage. Data will be written in the short term to hard disks in a RAID5 configuration and then

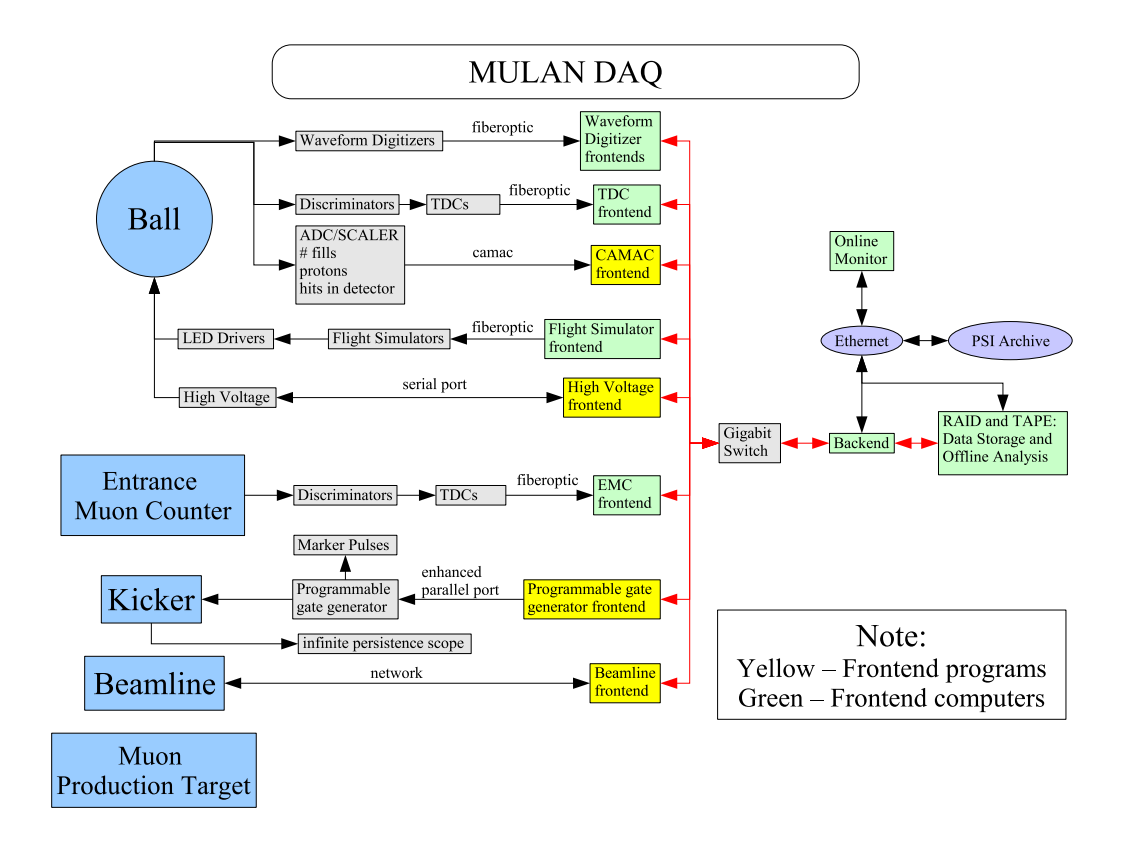


Figure 5: Overview of the MuLan data acquisition system. Data moves from hardware through the frontend computers to the backend computer. The backend stores the data and provides experiment control and online feedback to check detector health.

stored on tape. On overview of other DAQ systems providing experiment control and data readout is given in figure 5. We expect 10^{12} events to consume thirty terrabytes on tape.

VI. ANALYSIS

The MuLan analysis is done with a combination of MIDAS software for extracting the data from tape and ROOT for histogram display and fitting [9]. The analysis software attempts to fit

$$f(t) = N_0 e^{-t/\tau_{\mu}} + (\text{flat background})$$
 (5)

to the data using a χ^2 minimization,

$$\chi^2 = \sum_{k=1}^n \left(\frac{f(t_k) - f_k}{\sigma_k} \right)^2.$$

as shown in figure 6.

The analysis is blind because only collaboration members not involved in the analysis know the secret clock frequency offset. The analyzers only know the clock frequency to about 500 ppm. The

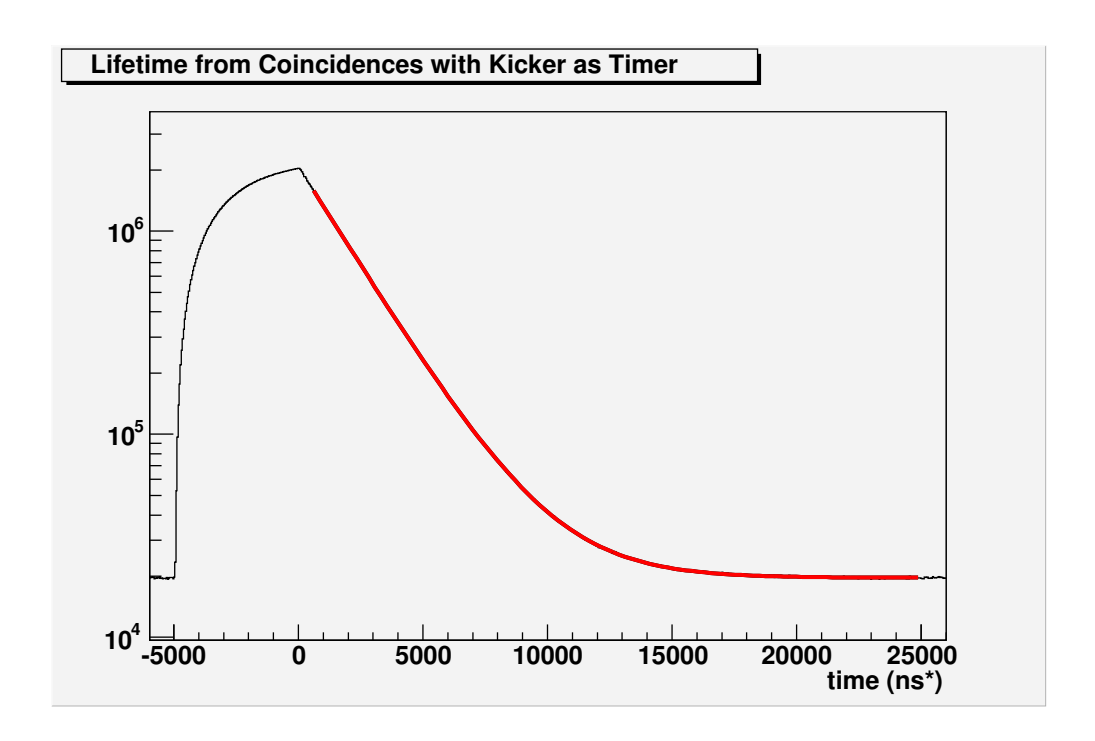


Figure 6: Sample lifetime plot from the Fall 2004 run on a sulfur target. The time structure introduced by the kicker is shown by the beam turn-on at -5000 ns, and the beam turn-off at 0 ns. A secret clock frequency offset introduces a shift of up to 500 ppm on the muon lifetime. The red line shows a simple three parameter fit to the data. This plot was made from one detector pair, representing $3\pi/170$ coverage of the target.

analysis may seem simple or straightforward, but part of the challenge inherent in high-precision measurements is gaining an understanding of the systematics at the 1 ppm level. The most dangerous systematic effects are those that occur on the timescale of the lifetime of the muon. These "early-to-late" effects distort the shape of the lifetime. If they are not identified and accounted for, they will distort the muon lifetime fit.

A. Pileup

A persistent problem with most detectors is the deadtime immediately following a hit. In the current TDC setup, the discriminators have a 10 ns deadtime, which results in the loss of the second event if two events occur within 10 ns of each other. This loss of events adds an exponential curve to the muon lifetime plot with characteristic time half that of the muon lifetime. Accurately knowing the amplitude of this effect, as opposed to fitting it, increases the statistical power of the fit. When the electronics are refitted with WFDs, pileup effects will be diminished but not eliminated. The WFDs digitize continually, but two pulses extremely close together will look like one large pulse. With WFDs, a pulse resolution of 4 ns is expected. The scintillator tile itself has no dead time, but

the zero-level of a second pulse is raised by a pulse immediately prior to it. Additionally, a prior pulse may affect the gain of a phototube if the high voltage power supply has not had a chance to recharge. The high segmentation of the detector and the fast electronics are designed to reduce pileup as much as possible.

B. Spin precession

"Surface muons" are produced from pion decay at rest at or near the surface of the carbon production target. Neutrino left-handedness and angular momentum conservation result in the muon spin pointing antiparallel to its momentum. The muon's helicity is preserved as it travels through the piE3 beamline until it stops in the MuLan target with its spin pointing upstream. Without a depolarizing target, the ensemble of muons is remains highly polarized. Since muon decay violates parity, positrons are emitted preferentially in the spin direction of the muon (Eq. 2). Free muons precess in a magnetic field with frequency

$$\omega/B = 8.5 \times 10^8 \text{rad/sT}$$

which corresponds to a revolution frequency of 13.5 kHz/G. The earth's magnetic field (0.5 G) results in a spin precession just enough to turn the preferred direction for muon decay by one detector tile during the muon's lifetime. Differences in gain between detector tiles will then result in a distortion of the lifetime. To counteract this effect, a depolarizing target is used, in combination with an externally applied magnetic field. By applying an external magnetic field, the precession frequency is increased until this effect becomes apparent as a wiggle superimposed on the muon lifetime. The symmetry of the detector also serves to counteract this effect, since lifetime histograms from opposite tile pairs can be summed to cancel the wiggle, or subtracted to enhance it for study.

C. Non-flat background

In pulsed-beam mode, the kicker is "off" for 5 μs allowing muons through and "on" for a measurement period of 27 μs to deflect incoming muons into the side of the beam pipe. During the run in the fall of 2004, we achieved an extinction factor, defined as

$$extinction factor = \frac{N_0}{\text{flat background}},$$

(ref: 5) of roughly 300. A non-flat background could arise from a changing kicker extinction factor or a time-dependent beam rate. A sloping or higher-order background term could distort the fit of

the muon lifetime.

D. Rare decays

There are two muon decay modes other than the dominant $\mu^+ \to e^+ + \nu_e + \bar{\nu}_\mu$ decay mode. The first is

$$\mu^+ \to e^+ + \nu_e + \bar{\nu}_\mu + \gamma$$

with branching ratio $1.4 \pm 0.4\%$. The second is

$$\mu^+ \to e^+ + e^+ + e^- + \nu_e + \bar{\nu}_\mu$$

with branching ratio $3.4 \pm 0.4 \times 10^{-5}$. The MuLan detector has a slight chance to observe the γ if it pair produces ($\gamma \to e^+e^-$) before it exits the inner scintillator tile, in which case there would be two recorded tile events for one muon decay. Likewise, when the second process takes place, it is possible that three events would be recorded for one muon decay. Fortunately, these processes do not distort the shape of the lifetime curve, since the branching ratio of these decays does not change on the timescale of the muon lifetime. These decays simply shift the statistical weight of a timing bin.

E. Other effects

Rate-dependent effects in the timing electronics would distort the lifetime. We are constructing an LED pulser system to fire at known intervals during data acquisition to check for timing distortions.

The phototubes used in the MuLan experiment were designed to reduce afterpulses caused by time-delayed cascades within the phototube. Empirically, an afterpulse appears as a smaller pulse after the main pulse. This may not distort the lifetime, but it would lower the statistical weight of the bins in the lifetime histogram and would therefore increase the χ^2 of the fit.

VII. PERSONAL CONTRIBUTION

My contributions to this experiment center around the data acquisition system. My first task was repairing a 256 channel phototube power supply and configuring its software drivers so it could be monitored and controlled though MIDAS. More recently, I implemented an upgrade of

the MIDAS software, which improved its functionality and reduced bugs. The upgrade process created incompatibilities between the MuLan DAQ software and the new MIDAS libraries that required significant understanding of both to resolve. Tangentally, I maintain the software archive and help coordinate the activity of other developers. I also manage the hardware and software analysis framework for parallel data analysis across multiple machines. I've written two analysis visualization tools to plot parameters vs. location on the ball and parameters vs. location in the TDCs. During the fall 2004 run, I helped identify problems with the software that were causing inconsistencies in the data (specifically, missing start words) and implemented a hardware DAQ synchronization using known-working code. Additionally, I've been investigating data formats and compression schemes for the eventual recording of 10^{12} events. I also assisted in the development and layout of the EMC readout boards, shown in green in figure 2. Once the EMC was complete, I conditioned it to high voltage and began testing its efficiency using a stripped-down data acquisition.

VIII. CONCLUSION

Most of the detector hardware is already in place, with the WFDs nearing completion. Given the fundamental nature of G_F and the fact that its currect uncertainty is entirely dependent on the experimental uncertainty on the muon lifetime, an updated measurement must be performed. All that is needed is a dedicated graduate student to push the experiment forward to the 1 ppm level.

Acknowledgments

Thanks to Professor David Hertzog and the MuLan collaboration for giving me this opportunity.

^[1] N. Danneberg et. al. Muon Decay: Measurement of the Transverse Polarization of the Decay Positrons and its Implications for the Fermi Coupling Constant and Time Reversal Invariance. *Phys. Rev. Lett.*, 94:021802, 2005.

^[2] S. Eidelman et. al. (Particle Data Group). Review of Particle Physics. Physics Letters B, 592:1+, 2004.

^[3] Y. Kuno and Y. Okada. Muon Decay and Physics Beyond the Standard Model. Rev. Mod. Phys., 73:151–202, 2001.

^[4] K. Lynch. Statistical Error Models for the μ Lan Experiment. μ Lan Note, 2003.

^[5] William J. Marciano. Fermi Constants and "New Physics". Phys. Rev. D, 60:093006, 1999.

- [6] T. van Ritbergen and R. G. Stuart. On the Precise Determination of the Fermi Coupling Constant from the Muon Lifetime. *Nucl. Phys. B*, 564:343–390, 2000.
- [7] CMP16F webpage. http://www-hep.phys.cmu.edu/cms/welcome.html.
- [8] MIDAS webpage. http://midas.psi.ch.
- $[9] \ \ ROOT \ webpage. \ http://root.cern.ch.$